Nonlinear analysis of an oscillating water column wave energy device in frequency domain via statistical linearization

Conference Paper · June 2019

CITATION
1

READS
261

4 authors:

Leandro Souza Pinheiro Da Silva
University of São Paulo
8 PUBLICATIONS **6** CITATIONS
SEE PROFILE

Celso P. Pesce
University of São Paulo
157 PUBLICATIONS **982** CITATIONS
SEE PROFILE

H. M. Morishita
University of São Paulo
57 PUBLICATIONS **257** CITATIONS
SEE PROFILE

Rodolfo Trentin Gonçalves
The University of Tokyo
112 PUBLICATIONS **632** CITATIONS
SEE PROFILE

Proceedings of the ASME 2019 38th International
Conference on Ocean, Offshore and Arctic Engineering
OMAE2019
June 9-14, 2019, Glasgow, Scotland, UK

OMAE2019-96727

NONLINEAR ANALYSIS OF AN OSCILLATING WATER COLUMN WAVE ENERGY DEVICE IN FREQUENCY DOMAIN VIA STATISTICAL LINEARIZATION

Leandro S.P. da Silva*
Escola Politécnica
Dept. of Naval Architecture and Ocean Engineering
University of São Paulo
Butantã, São Paulo, Brazil 05508-010

Celso P. Pesce
Escola Politécnica
Offshore Mechanics Laboratory
University of São Paulo
Butantã, São Paulo, Brazil 05508-010

Helio M. Morishita
Escola Politécnica
Dept. of Naval Architecture and Ocean Engineering
University of São Paulo
Butantã, São Paulo, Brazil 05508-010

Rodolfo T. Gonçalves
School of Engineering
Dept. of Systems Innovation
The University of Tokyo
Tokyo, Japan, 113-8656

ABSTRACT

Wave energy converters (WECs) are often subject to large displacements during operating conditions. Hence, nonlinearities present in numerical methods to estimate the performance of WECs must be considered for realistic predictions. These large displacements occur when the device operates on resonant conditions, which results in maximum energy conversion. The system dynamics are usually simulated via time domain models in order to being able to capture nonlinearities. However, a high computational cost is associated with those simulations. Alternatively, the present work treats the nonlinearities in the frequency domain via Statistical Linearization (SL). The SL results are compared to the Power Spectrum Density (PSD) of time domain simulations to verify the reliability of the proposed method. In this regard, the work initiates with the derivation of the governing equations of the air-chamber and the Oscillating Water Column (OWC). Then, the SL technique is presented and applied. The SL results show a satisfactory agreement for the system dynamics, mean surface elevation, mean pressure, and mean power compared to time domain simulations. Also, the SL technique produces a rapid estimation of the response, which is an effective approach for the evaluation of numerous environmental conditions and design, and further optimization procedures.

INTRODUCTION

The exploitation of renewable sources of energy has been driven to meet the continuous growth of global energy demand. The benefits of those sources range from the vast amount of energy to its environmentally friendly characteristics. Among the renewable sources, wave energy has been insufficiently explored and has a promising capability to contribute to the energy industry. Ocean waves have a substantial amount of power, which are estimated to be more than 2 TW globally [1]. Moreover, the regularity in the energy distribution [2] and spatial concentration also promotes the use of wave energy as a source of energy [3]. As a result, the interest in wave energy by industry and the scientific community has intensified. Currently, several wave absorption

*Address all correspondence to this author: Leandropinheiro@usp.br.

mechanisms have been proposed [4, 3], in which only a limited number have become feasible and installed [5]. Between the options, this work investigates the OWC wave energy device.

The concept of the OWC as a wave energy device was firstly developed by Yoshio Masuda in the 1940s. Since then, several OWC prototypes have been operating in many places in the world [4]. Typically, OWCs are composed of a fixed or floating hollow structure, which acts as a chamber. The base of the structure is open to the sea, and it is located below the water surface. On these devices, the wave action leads the inner free surface to oscillate, which compresses and decompresses the air inside the chamber. This mechanism forces the air to move back and forth through a turbine connected to a generator that converts the kinetic energy of the moving flow into electricity. Generally, bidirectional turbines are employed, such as Wells turbines. The main components of an OWC and its working principle are illustrated in Figure 1.

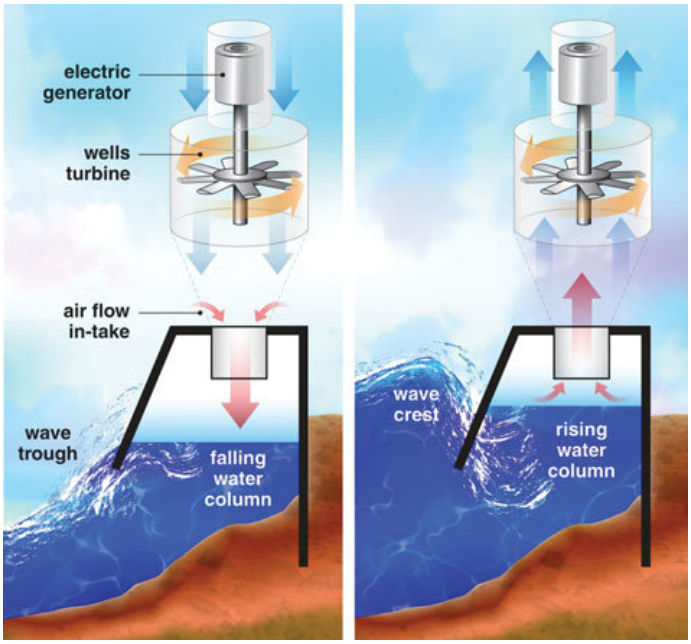

FIGURE 1: OSCILLATING WATER COLUMN WAVE ENERGY DEVICE [6]

The feasibility of energy devices depends on the efficiency of the entire system. From the hydro-mechanical point of view, a key to a good performance occurs when the water column resonates with the wave loads. For such conditions, nonlinearities play an important role in the system dynamics. Therefore, an appropriate modeling is required to optimize the power extraction and for a better understanding of the physics. Hence, prior to the application of the SL technique, the governing equations are derived.

OWC WAVE ENERGY DEVICE MODELING

Consider a fixed box-shaped structure piercing a quiescent free surface, which acts as a chamber. The mass inside the chamber (m_{ch}) is defined by a control volume, being composed of a water column (m_w) and air mass (m_{air}). As the inner free surface is free to move, the mass in the control volume varies as:

$$m_{ch} = m_w + m_{air}, \tag{1}$$

where:

$$m_w = \rho_w S(H + \zeta), \tag{2}$$

$$m_{air} = \rho_{air} S(L - \zeta). \tag{3}$$

The nominal draft is denoted by H, the air-chamber height at the nominal position is L, the air density varies due compressibility effects and is given by ρ_{air}, and the cross section area of the chamber is S (see Figure 2). The water is assumed incompressible and inviscid. However, note that the effect of the viscous drag force may be further included, in an ad-hoc manner, in the OWC dynamics. As can be observed in Eqs. (2) and (3), the mass inside the chamber has an explicit dependency on the position of the inner free surface, here denoted by $\zeta(t)$. The description of the problem and some components are illustrated in Figure 2.

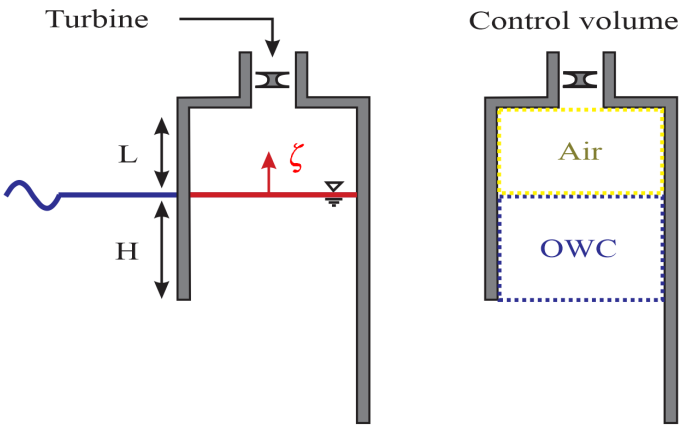

FIGURE 2: DESCRIPTION OF THE SYSTEM

Taking the time derivative of the mass functions, Eqs. (2)

and (3), the mass flux rate inside the chamber is obtained.

$$\dot{m}_{ch} = \dot{m}_w + \dot{m}_{air},$$

$$\dot{m}_w = \rho_w S\dot{\zeta}, \tag{4}$$

$$\dot{m}_{air} = -\dot{m}_{turb} = -\rho_{air} S\dot{\zeta} + \dot{\rho}_{air} S(L-\zeta), \tag{5}$$

where $\dot{m}_{air}$ represents the mass flow rate of air that passes through the turbine and produces energy. Note that $\dot{m}_{turb}$ is defined positive for outward flow from the chamber. The mass flux and pressure are related by the air turbine. To simplify the physics behind the aerodynamics of air turbines, the turbine's performance is presented in terms of coefficients in dimensionless form [7]:

$$\Phi = f_Q(\Psi), \tag{6}$$

$$\Pi = f_p(\Psi), \tag{7}$$

where

$$\Psi = \frac{p}{\rho_{in} N^2 D^2}, \tag{8}$$

$$\Phi = \frac{\dot{m}_{turb}}{\rho_{in} N D^3}, \tag{9}$$

$$\Pi = \frac{P_{turb}}{\rho_{in} N^3 D^5}, \tag{10}$$

where Ψ, Φ, Π are the dimensionless parameters of: pressure head, flow rate, and power coefficient respectively. N denotes the turbine rotational speed (rad/s), D is the rotor diameter, p is the manometric pressure, ρ_{in} is the air density in stagnation conditions at the turbine entrance, here assumed equal to ρ_{air}.

Considering the case of Wells turbines, the mass flow rate and the pressure fluctuation present an approximately linear relationship [8], $\Phi = K\Psi$. Therefore, in dimensional form, the mass flow rate can be related to the pressure by:

$$\dot{m}_{turb} = \frac{KD}{N} p, \tag{11}$$

where K is the proportionality constant. The air inside the chamber is assumed to behave as an isentropic process [9]:

$$\dot{\rho}_{air} = \frac{1}{c_a^2}\dot{p}, \tag{12}$$

where c_a is the speed of sound in atmospheric conditions. Therefore, based on the assumption described, the pressure can be written as:

$$\rho_{air} S\dot{\zeta} = \frac{KD}{N} p + \frac{S}{c_a^2}(L-\zeta)\dot{p}. \tag{13}$$

Regarding the dynamics of the water column, the simplest model may be then given by a single degree of freedom system based on a plug-flow representation, through the generalized coordinate zeta. In this work, the water column dynamic is based on the derivations described in [10], which for a non-forced system and without dissipative forces is given by:

$$\rho_w S(\zeta + H)\ddot{\zeta} + \frac{1}{2}\rho_w S\dot{\zeta}^2 + \rho_w S g\zeta = 0. \tag{14}$$

This equation was obtained by two distinct approaches: via the extended Lagrange equations applied to variable mass systems; and via classical hydrodynamic techniques, taking into account the momentum and the flux in the non-material control surface; see in [11, 12].

Three non-conservative forces are incorporated in the oscillating water column dynamics, classified as: (i) the excitation force due to the waves, f_{exc}, at the control surface on the water column mouth (a non-material surface); (ii) the force caused by the air-chamber pressure acting on the free-surface (a material interface), f_{ch}; and (iii) and an ad-hoc assumed parcel due to viscous effects (caused by vortical flow at the mouth), f_v.

$$f^{nc} = f_{exc} + f_{ch} + f_v. \tag{15}$$

Under the assumption of the linear wave theory, considering a reflective wave and a uniform wave pressure all over the control surface at the water column mouth, the wave excitation force can be written as [13]:

$$f_{ext} = 2A\rho_w g S\cos(kx - \omega t)\frac{\cosh(k(h-H))}{\cosh(kh)}, \tag{16}$$

where A denotes the wave amplitude, h is the considered water depth, g is the gravitational acceleration and k is the wavenumber

given by:

$$k = \frac{\omega^2}{g\tanh(kh)}. \tag{17}$$

Regarding the air-chamber model, the pressure exerts a force on the free-surface equivalent to:

$$f_{ch} = -Sp. \tag{18}$$

The ad-hoc viscous flow effects can be modeled as:

$$f_v = -\frac{1}{2}C_v\rho_w S\dot{\zeta}|\dot{\zeta}|, \tag{19}$$

where C_v denotes the viscous coefficient.

Based on the non-conservative forces terms assumed, the resulting governing equation for the OWC is given by:

$$(\zeta + H)\ddot{\zeta} + \frac{1}{2}\dot{\zeta}^2 + \frac{1}{2}C_v\dot{\zeta}|\dot{\zeta}| + g\zeta + \frac{1}{\rho_w}p = F_{ext} \tag{20}$$

with:

$$F_{ext} = f_{ext}/(\rho_w S).$$

Regarding the governing equation of the air-chamber pressure, rearranging Eq. (13) yields:

$$\frac{KD}{NS}p + \frac{1}{c_a^2}(L-\zeta)\dot{p} - \rho_{air}\dot{\zeta} = 0. \tag{21}$$

Besides the governing equations, the analysis of wave energy devices relies on the estimation of the power produced. Based on Eqs. (7) and (10), the instantaneous power output of the air turbine is [8]:

$$P_t(t) = \rho_{air}N^3D^5 f_p\left(\frac{p(t)}{\rho_{air}N^2D^2}\right). \tag{22}$$

Therefore, in a period T of time, the mean power is given by:

$$\bar{P}_t = \frac{\rho_{air}N^3D^5}{T}\int_{t_0}^{t_0+T} f_p\left(\frac{p(t)}{\rho_{air}N^2D^2}\right)dt. \tag{23}$$

STATISTICAL LINEARIZATION

This section deals with the modeling in Frequency Domain (FD) via SL technique for the OWC. The technique allows a reliable prediction of the WEC dynamics and power output [14], which can be a valuable tool for the assessment of several design and environmental conditions, and further optimization procedures [15]. The SL procedure employed in this work is developed based on Robert and Spanos [16]. Consider a general multi-degrees-of-freedom nonlinear equation:

$$\mathbb{M}\ddot{\mathbf{q}} + \mathbb{B}\dot{\mathbf{q}} + \mathbb{K}\mathbf{q} + \Theta(\mathbf{q},\dot{\mathbf{q}},\ddot{\mathbf{q}}) = \mathbf{F}, \tag{24}$$

where $\mathbb{M}$, $\mathbb{B}$ and $\mathbb{K}$ are the mass, damping and stiffness $n\times n$ matrices, and Θ denotes a nonlinear n-vector function, which depends on the generalized coordinated n-vector $\mathbf{q}$ and its respective time derivatives. The SL-equivalent linear system of Eq.(24) is defined as:

$$(\mathbb{M}+\mathbb{M}_{eq})\ddot{\mathbf{q}} + (\mathbb{B}+\mathbb{B}_{eq})\dot{\mathbf{q}} + (\mathbb{K}+\mathbb{K}_{eq})\mathbf{q} = \mathbf{F}, \tag{25}$$

where $\mathbb{M}_{eq}$, $\mathbb{B}_{eq}$ and $\mathbb{K}_{eq}$ represents the equivalent linear mass, damping and stiffness matrices.

An additional treatment is required for the SL technique, due to the source of nonlinearity described in Eqs. (20) and (21), which result in a constant offset in the system solutions. Based on that, the system can be written in terms of a mean value, $(\bar{\cdot})$ and a random zero mean component of the response $(\hat{\cdot})$:

$$\mathbf{q}(\mathbf{t}) = \bar{\mathbf{q}} + \hat{\mathbf{q}}(\mathbf{t}). \tag{26}$$

Hence, considering a zero-mean force, Eq. (24) can be written as:

$$\mathbb{M}\ddot{\hat{\mathbf{q}}} + \mathbb{B}\dot{\hat{\mathbf{q}}} + \mathbb{K}\bar{\mathbf{q}} + \mathbb{K}\hat{\mathbf{q}} + \Theta(\bar{\mathbf{q}}+\hat{\mathbf{q}},\dot{\hat{\mathbf{q}}},\ddot{\hat{\mathbf{q}}}) = \hat{\mathbf{F}}. \tag{27}$$

The equilibrium is estimated taking the expectation of Eq. (27):

$$\mathbb{K}\hat{\mathbf{q}} + \left\langle \Theta(\bar{\mathbf{q}}+\hat{\mathbf{q}},\dot{\hat{\mathbf{q}}},\ddot{\hat{\mathbf{q}}}) \right\rangle = 0, \tag{28}$$

where, $\langle . \rangle$ denotes the mathematical expectation. Subtracting Eq. (28) from Eq. (27), a similar form of Eq. (24) is obtained:

$$\mathbb{M}\ddot{\hat{\mathbf{q}}} + \mathbb{B}\dot{\hat{\mathbf{q}}} + \mathbb{K}\bar{\mathbf{q}} + G(\hat{\mathbf{q}},\dot{\hat{\mathbf{q}}},\ddot{\hat{\mathbf{q}}}) = \hat{\mathbf{F}}, \tag{29}$$

where,

$$\mathbf{G}(\hat{\mathbf{q}},\dot{\hat{\mathbf{q}}},\ddot{\hat{\mathbf{q}}}) = \Theta(\bar{\mathbf{q}}+\hat{\mathbf{q}},\dot{\hat{\mathbf{q}}},\ddot{\hat{\mathbf{q}}}) - \left\langle \Theta(\bar{\mathbf{q}}+\hat{\mathbf{q}},\dot{\hat{\mathbf{q}}},\ddot{\hat{\mathbf{q}}}) \right\rangle.$$

The equivalent linear terms in Eq. (25) are determined by minimizing the mean square difference between the the nonlinear function and the equivalent linear system based on a statistical point of view. Assuming a Gaussian response distribution and minimizing the difference between the nonlinear and the equivalent linear equations in a mean square sense, the equivalent linear terms are obtained by:

$$M_{eq_{i,j}} = \left\langle \frac{\partial G_i}{\partial \ddot{q}_j} \right\rangle, \tag{30}$$

$$B_{eq_{i,j}} = \left\langle \frac{\partial G_i}{\partial \dot{q}_j} \right\rangle, \tag{31}$$

$$K_{eq_{i,j}} = \left\langle \frac{\partial G_i}{\partial q_j} \right\rangle, \tag{32}$$

where $M_{eq_{i,j}}, B_{eq_{i,j}}, K_{eq_{i,j}}$, are i, j elements of the equivalent mass, damping and stiffness matrix respectively.

The response is assumed Gaussian due to a random phase relationship between the wave force components [8], which is given by:

$$f(\mathbf{q}) = \frac{1}{(2\pi)^{n/2}|\mathbb{V}|^{1/2}} \exp\left(-\frac{1}{2}(\hat{\mathbf{q}} - \bar{\mathbf{q}})^{\mathrm{T}} \mathbb{V}^{-1} (\hat{\mathbf{q}} - \bar{\mathbf{q}}) \right), \tag{33}$$

where $\mathbb{V}$ is the covariance matrix of $\mathbf{q}$, and $|\mathbb{V}|$ denotes the determinant of the covariance matrix.

According to Eqs. (30 - 32), the equivalent terms require the information of the response distribution. Since no analytic solution is available, the SL method consists of an iterative procedure. As an initial guess, the linearized system is considered based on Eqs.(20) and (21) :

$$H\ddot{\zeta} + g\zeta + \frac{1}{\rho_w} p = F_{ext}, \tag{34}$$

$$\frac{KD}{NS} p + \frac{L}{c_a^2} \dot{p} - \rho_{air} \dot{\zeta} = 0. \tag{35}$$

Hence, the frequency response function of the linear system is given by:

$$\alpha(\omega) = [-\omega^2(\mathbb{M}) + i\omega(\mathbb{B}) + (\mathbb{K})]^{-1}. \tag{36}$$

The response matrix is computed as:

$$S_q(\omega) = \alpha(\omega) S_F(\omega) \alpha^{\mathrm{T}}(\omega), \tag{37}$$

where $(\,)^{\mathrm{T}}$ denotes the transpose conjugate of a matrix, and $S_F(\omega)$ is the power spectrum of the excitation. Based on the response matrix, the mean values of the generalized coordinates are calculated using Eq. (28), which for the pressure is given by:

$$\frac{KD}{NS} \bar{p} - \frac{1}{c_a^2} \langle \zeta \dot{p} \rangle = 0, \tag{38}$$

and for the water column is given by:

$$\langle \zeta \ddot{\zeta} \rangle + \frac{1}{2} \langle \dot{\zeta}^2 \rangle + g\bar{\zeta} + \frac{1}{\rho_w} \bar{p} = 0. \tag{39}$$

Further, the equivalent linear terms, Eqs. (30 - 32) are calculated. The frequency response function is updated containing the equivalent terms:

$$\alpha(\omega) = [-\omega^2(\mathbb{M} + \mathbb{M}_{eq}) + i\omega(\mathbb{B} + \mathbb{B}_{eq}) + (\mathbb{K} + \mathbb{K}_{eq})]^{-1}, \tag{40}$$

and the iterative procedure continues until convergence. Once the convergence is achieved, based on Eq. (23), the mean power estimation in the frequency domain can be determined as:

$$\bar{P}_t = \rho_{air} N^3 D^5 \left\langle f_p \left(\frac{p(t)}{\rho_{air} N^2 D^2} \right) \right\rangle, \tag{41}$$

where $p(t)$ is composed of a non-zero mean and a random zero mean component.

SIMULATIONS

In this section, the reliability of the SL technique is verified comparing its results with those from nonlinear time domain simulations. For the excitation force, the waves were described by a JONSWAP spectrum with significant wave height (H_s) of 1.5m, peak enhancement factor (γ) of 3.3, and the peak period (T_p) was varied from 4 to 10s, which are values typical from the Scotland/EMEC test site [17]. Based on that, the natural frequency of the OWC, which considers small displacements,

$$\omega_n = \sqrt{\frac{g}{H}}, \tag{42}$$

was set to operate between the range of the wave peak frequencies (natural period, $T_n = 5.68$s). However, note that the conditions simulated are illustrative, the mean power of the operating conditions were not optimized. The simulation parameters are described in Table 1.

TABLE 1: SIMULATION PARAMETERS.

Property	Value	Unit
ρ_w	1025	$[\mathrm{kg/m^3}]$
ρ_{air}	1.25	$[\mathrm{kg/m^3}]$
C_v	0.5	$[-]$
K	0.28	$[-]$
H	8	[m]
D	1.75	[m]
L	9	[m]
h	50	[m]
S	10	$[\mathrm{m^2}]$
N	30	[rad/s]
c_a	344	[m/s]
g	9.81	$[\mathrm{m/s^2}]$
ω_n	1.107	[rad/s]
T_n	5.68	[s]

In this work, the frequency domain label (FD) refers to the linearized system around its equilibrium condition, Eqs. (34) and (35), which are used for the initial guess in the SL technique. This nomenclature will be used during the discussion of the results.

Figures 3 and 4 show the PSD results at the water column resonance for the water surface elevation and pressure using the different approaches. The PSD of time domain simulations were calculated using the *pwelch* function in MATLAB, in which the data were acquired during a period larger than of 25000 cycles to guarantee ergodicity. Figure 5 shows the probability density function (PDF) of the pressure at resonance. Note that the assumption of a Gaussian distribution recovers the results coming from the time simulation data, preserving the standard deviation. This similarity occurs for the other conditions simulated. Figure 6 shows the PSD for several wave peak periods, (from $T_p = 4$ to 10s).

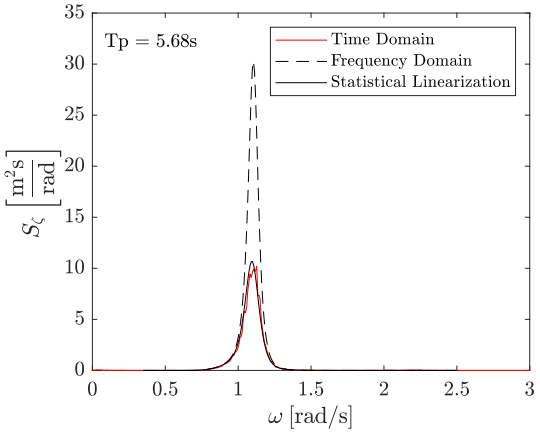

FIGURE 3: PSD OF THE WATER COLUMN DISPLACEMENT AT RESONANCE

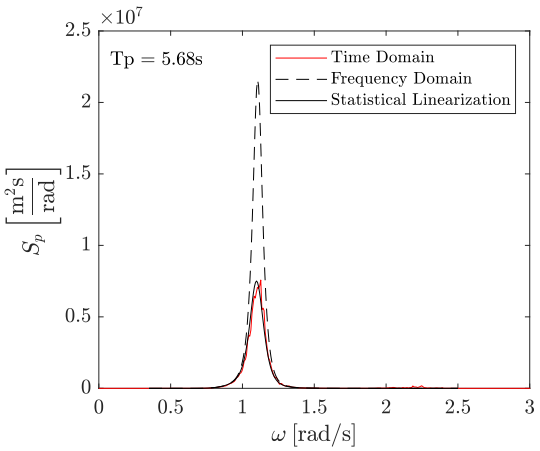

FIGURE 4: PSD OF THE AIR-CHAMBER PRESSURE AT RESONANCE

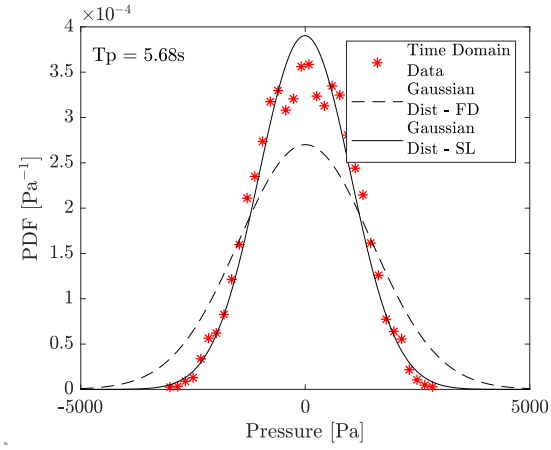

FIGURE 5: PDF OF THE PRESSURE AT RESONANCE.

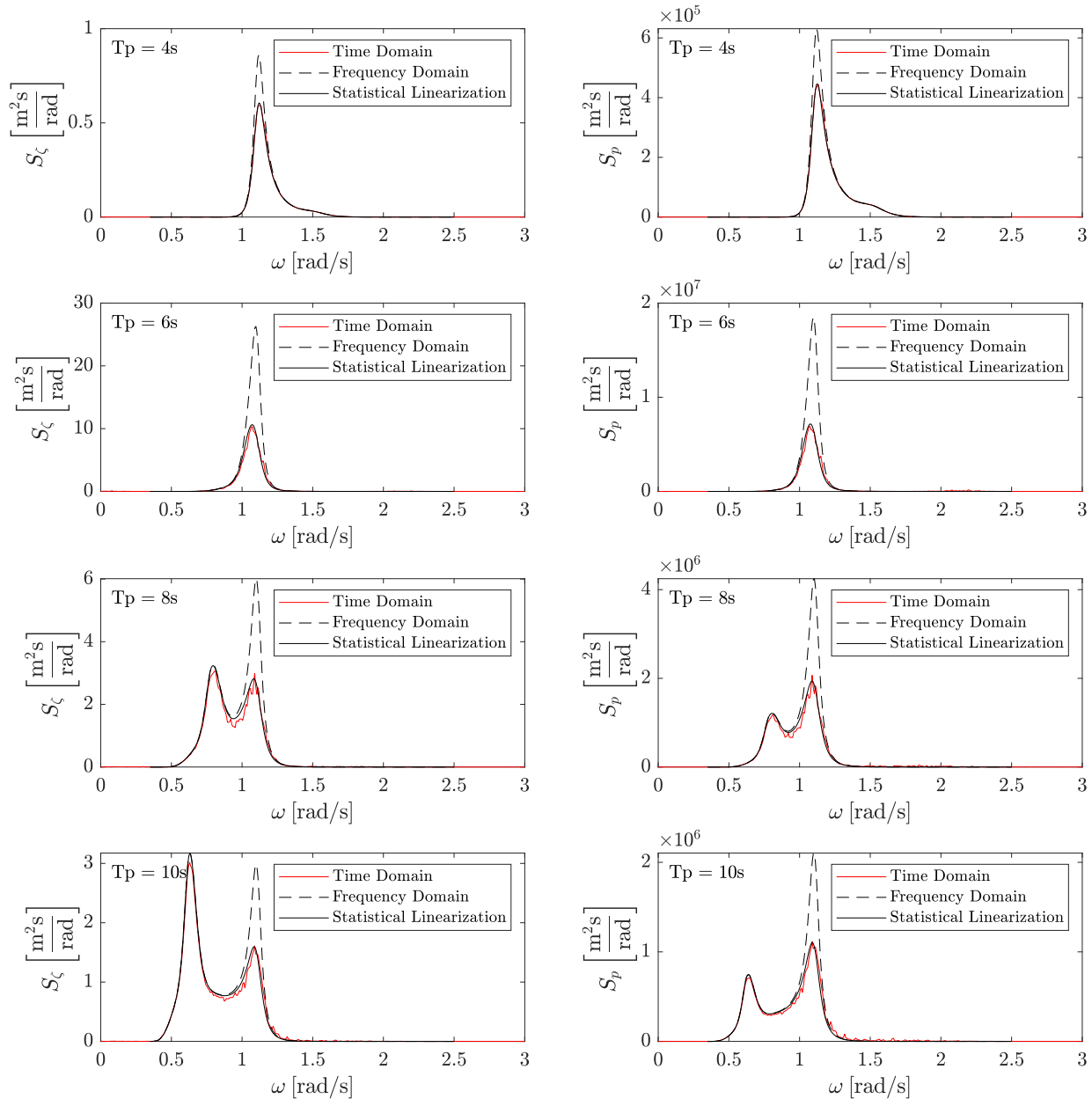

FIGURE 6: PSD FOR SEVERAL JONSWAP PEAK-PERIODS (T_p); LEFT: WATER COLUMN DISPLACEMENT (ζ); RIGHT: AIR-CHAMBER PRESSURE (p)

As expected, the water column displacement is amplified at the natural frequency for all conditions. The OWC response is dominated by the damping and nonlinear terms with velocity dependency for the resonance regime. Also, the response of the system can vary according to the source of nonlinearities and the ratio between the linear and nonlinear forces. For instance, the reduction of the OWC draft increases the natural frequency of the water column, and the nonlinearities with acceleration and velocity dependency become more relevant for regions with higher frequencies. For this case, the SL-equivalent linear system might shift the response peak frequency for more severe wave conditions.

In Figs. 7 and 8, as the frequency-domain analysis is not able to estimate the mean pressure and mean displacement, only the SL and time domain results are presented, which uses Eqs. (38) and (39). The mean power obtained from time domain simulations was calculated according to Eq. (23), while for the SL and the linear frequency domain was calculated using Eq. (41); (see Fig 9). The air turbine coefficients were taken from [7]. As the viscous force dissipates part of the energy, especially for higher displacements at resonant condition, the prediction using the standard frequency domain approach overestimates the mean power produced.

As it can be noticed in Figs. 3 to 9, the SL results have shown a good agreement compared to their equivalent nonlinear time domain simulations in terms of PSD, mean water column displacement, mean pressure, and mean power. However, it is valuable to mention that the SL technique required a less computational effort compared to the time domain simulations, converging in few iterations.

CONCLUSION

Wave energy devices usually operate next to resonant conditions leading to large displacements. As a result, non-linearities play an important role and must be included in the dynamic model that describes the system. In this regard, this work initiates with the nonlinear modeling of an OWC wave energy device using a simple two-degrees-of-freedom system: (i) one to describe the nonlinear behavior of the air-chamber and turbine, and (ii) one to describe the OWC dynamics. Subsequently, the SL technique is presented and applied to the system. The reliability of the method was assessed by comparing results with those coming from direct time domain simulations, with a very good agreement. As the number of variables for optimizing the OWC is large, the method employed in this work offers a valuable approach for further assessment of several conditions and designs to obtain a better performance of the wave energy device. The computational cost associated with those simulations are relatively smaller when compared to time domain simulations, with very good results in terms of PSD, mean water elevation, mean pressure, and mean power.

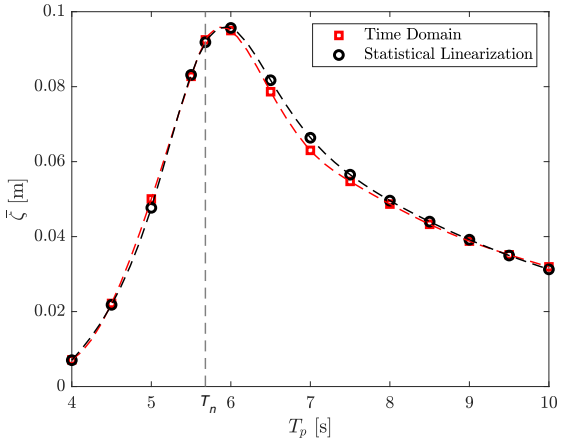

FIGURE 7: MEAN DISPLACEMENT OF THE OWC

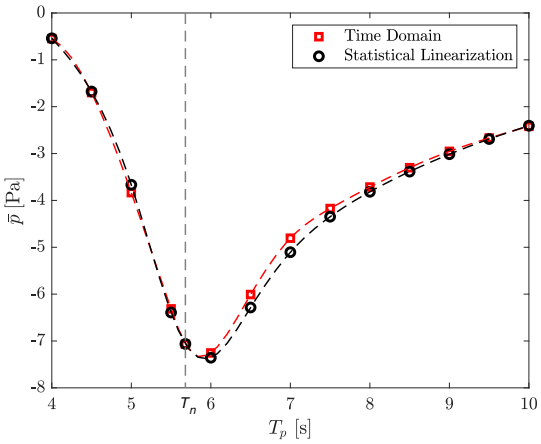

FIGURE 8: MEAN MANOMETRIC PRESSURE

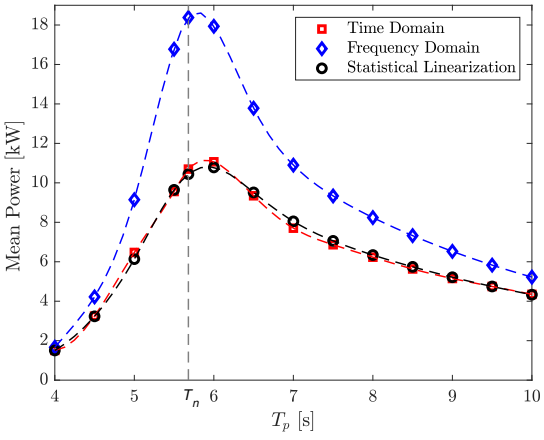

FIGURE 9: MEAN POWER

ACKNOWLEDGMENT

Leandro S. P. da Silva acknowledges CAPES, the Coordination for the Improvement of Higher Education Personnel, for his Master grant - Process number 1754875. C.P. Pesce acknowledges a CNPq Research Grant, nr. 308990/2014-5. The authors are grateful to the Wave Energy Group at The University of Adelaide for assisting this work.

REFERENCES

[1] Cruz, J., 2007. *Ocean wave energy: current status and future prespectives*. Springer Science & Business Media.

[2] Pelc, R., and Fujita, R. M., 2002. "Renewable energy from the ocean". *Marine Policy,* ***26***(6), pp. 471–479.

[3] Falnes, J., 2007. "A review of wave-energy extraction". *Marine Structures,* ***20***(4), pp. 185–201.

[4] Antonio, F. d. O., 2010. "Wave energy utilization: A review of the technologies". *Renewable and Sustainable Energy Reviews,* ***14***(3), pp. 899–918.

[5] Karimirad, M., 2014. *Offshore energy structures: for wind power, wave energy and hybrid marine platforms*. Springer.

[6] Muljadi, E., and Yu, Y.-H., 2015. "Review of marine hydrokinetic power generation and power plant". *Electric Power Components and Systems,* ***43***(12), pp. 1422–1433.

[7] Henriques, J., Portillo, J., Gato, L., Gomes, R., Ferreira, D., and Falcão, A., 2016. "Design of oscillating-water-column wave energy converters with an application to self-powered sensor buoys". *Energy,* ***112***, pp. 852–867.

[8] de O Falcão, A., and Rodrigues, R., 2002. "Stochastic modelling of OWC wave power plant performance". *Applied Ocean Research,* ***24***(2), pp. 59–71.

[9] Martins-Rivas, H., and Mei, C. C., 2009. "Wave power extraction from an oscillating water column at the tip of a breakwater". *Journal of Fluid Mechanics,* ***626***, pp. 395–414.

[10] Pesce, C. P., and Casetta, L., 2014. "Systems with mass explicitly dependent on position". In *Dynamics of mechanical systems with variable mass*. Springer, pp. 51–106.

[11] Pesce, C., 2003. "The application of Lagrange equations to mechanical systems with mass explicitly dependent on position". *Journal of Applied Mechanics,* ***70***(5), pp. 751–756.

[12] Pesce, C. P., Tannuri, E. A., and Casetta, L., 2006. "The Lagrange equations for systems with mass varying explicitly with position: some applications to offshore engineering". *Journal of the Brazilian Society of Mechanical Sciences and Engineering,* ***28***(4), pp. 496–504.

[13] Simonetti, I., Cappietti, L., El Safti, H., and Oumeraci, H., 2015. "Numerical modelling of fixed oscillating water column wave energy conversion devices: toward geometry hydraulic optimization". In ASME 2015 34th International Conference on Ocean, Offshore and Arctic Engineering, American Society of Mechanical Engineers, pp. V009T09A031–V009T09A031.

[14] Silva, L. S. P., Morishita, H. M., Pesce, C. P., and Gonçalves, R. T., 2019. "Nonlinear analysis of a heaving point absorber in frequency domain via statistical linearization". In ASME 2019 38th International Conference on Ocean, Offshore and Arctic Engineering, American Society of Mechanical Engineers.

[15] Silva, L. S. P., Tancredi, T. P., Ding, B., Sergiienko, N., and Morishita, H. M., 2017. "Fully submerged point absorber in Santa Catarina, Brazil - a feasibility study". In 24th ABCM International Congress of Mechanical Engineering (COBEM 2017).

[16] Roberts, J. B., and Spanos, P. D., 2003. *Random vibration and statistical linearization*. Courier Corporation.

[17] Nielsen, K., and Pontes, T., 2010. "Generic and site-related wave energy data". *Report T02-1.1 OES IA Annex II Task,* ***1***.